Identified particle spectra and anisotropic flow in an event-by-event hybrid approach in Pb + Pb collisions at sqrt[s_{NN}]=2.76TeV

Hannah Petersen

Phys. Rev. C **84**, 034912 — Published 27 September 2011

DOI: 10.1103/PhysRevC.84.034912

Identified Particle Spectra and Anisotropic Flow in an Event-by-Event Hybrid Approach in Pb+Pb collisions at $\sqrt{s_{\rm NN}} = 2.76$ TeV

Hannah Petersen
Department of Physics, Duke University, Durham, North Carolina 27708-0305, United States

The first results from heavy ion collisions at the Large Hadron Collider for charged particle spectra and elliptic flow are compared to an event-by-event hybrid approach with an ideal hydrodynamic expansion. This approach has been shown to successfully describe bulk observables at RHIC. Without changing any parameters of the calculation the same approach is applied to Pb+Pb collisions at $\sqrt{s_{\rm NN}} = 2.76$ TeV. This is an important test if the established understanding of the dynamics of relativistic heavy ion collisions is also applicable at even higher energies. Specifically, we employ the hybrid approach with two different equations of state and the pure hadronic transport approach to indicate sensitivities to finite viscosity. The centrality dependence of the charged hadron multiplicity, p_T spectra and differential elliptic flow are shown to be in reasonable agreement with the ALICE data. Furthermore, we make predictions for the transverse mass spectra of identified particles and triangular flow. The eccentricities and their fluctuations are found to be surprisingly similar to the ones at lower energies and therefore also the triangular flow results are very similar. Any deviations from these predictions will indicate the need for new physics mechanisms responsible for the dynamics of heavy ion collisions.

PACS numbers: 25.75.-q,24.10.Lx,24.10.Nz

Recently, the first results from heavy ion collisions at $E_{\rm cm} = 2.76A$ TeV have been published by the ALICE collaboration [1–4]. To study strongly interacting matter at high temperatures has been the goal of the relativistic heavy ion program at the Relativistic Heavy Ion Collider (RHIC) since more than a decade. The 10 times higher beam energies at the Large Hadron Collider (LHC) allow for the investigation of the dynamical evolution of nucleus-nucleus collisions that have been established in Au+Au collisions at $E_{\rm cm} = 200A$ GeV in a different kinematic range [5]. It is especially interesting, if the matter still behaves as a almost perfect liquid or if the quark gluon plasma becomes more viscous by going to higher temperatures [6–9].

Hybrid approaches that are based on hydrodynamics for the hot and dense stage of the evolution that is coupled to hadronic transport approaches to describe the successive decoupling of the matter have been very successful in describing the properties of the bulk matter that is created at RHIC [10–13] and LHC [14, 15]. Within the last year, full event-by-event hydrodynamic approaches [16–21] have become more favorable because it has turned out that the effect of initial state fluctuations on final flow observables needs to be studied in a consistent way to draw quantitative conclusions for e.g the value of the shear viscosity [22].

It is important to apply well-established approaches for the dynamical evolution of heavy ion reactions at RHIC to the higher energy collisions at LHC without tuning parameters to investigate how good the energy dependence is described by a specific model. Differences between the experimental data and the theoretical calculations imply the need for new physics concepts to be applied. To understand the bulk evolution at LHC energies is a prerequisite for all further detailed studies of e.g. jet quenching and energy loss or electromagnetic probes [23, 24].

In this manuscript a event-by-event hybrid approach based on the Ultra-relativistic Quantum Molecular Dynamics (UrQMD) transport approach with an embedded (3+1) dimensional ideal hydrodynamic evolution is applied to lead-lead collisions at LHC energies. First, a comparison to the available experimental data on charged particle multiplicities, p_T spectra and elliptic flow is carried out with the exact same parameter set that has been applied at RHIC energies. Then, transverse mass spectra and triangular flow for identified particles are predicted. To compare the amount of initial state fluctuations, the probability distributions of coordinate space eccentricities are compared to their corresponding values at RHIC.

Let us start with a short description of the hybrid approach that has been developed for SPS energies [18] and recently successfully applied to gold-gold collisions at the highest RHIC energy [25–27]. The early non-equilibrium evolution is described by the UrQMD approach [28, 29], where the two lead nuclei are initialized according to Wood-Saxon profiles followed by binary interactions of the nucleons. The main contribution to the particle production at high energies is achieved by string excitation and fragmentation where the hard collisions (momentum transfer $Q > 1.5$ GeV) are treated by PYTHIA [30–32].

At the so called starting time of $t_{\rm start} = 0.5$ fm the particle distributions are transferred to energy, momentum and net baryon density distributions by representing each particle with a three-dimensional Gaussian distribution (width $\sigma = 1$ fm) that is Lorentz-contracted along the beam direction. During the following ideal relativistic one fluid evolution [33, 34] two different equations of state are employed, one representing a hadron gas (HG-EoS) and one including a cross-over deconfinement phase transition based on a chiral approach (DE-EoS)[35–37]. The transition back to the hadronic transport approach happens on a constant proper time hypersurface, where

the Cooper-Frye equation is applied on transverse slices of thickness $\Delta z = 0.1 - 0.2$ fm that have cooled down below an energy density of ≈ 730 MeV/fm^3 [38]. This approach provides the full final phase space distributions of the produced particles for each event and can be compared to the pure transport approach by turning off the hydrodynamic evolution which allows for a qualitative study of viscous effects.

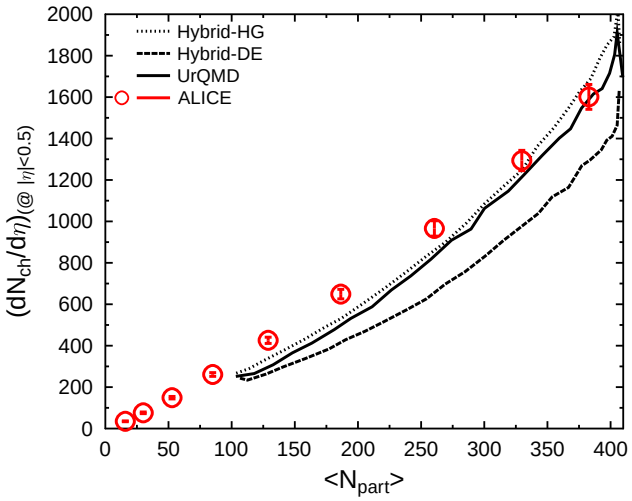

FIG. 1: (Color online) Charged particle multiplicity at midrapidity ($|\eta| < 0.5$) as a function of the number of participants in Pb+Pb collisions at $\sqrt{s_{\rm NN}} = 2.76$ TeV calculated in the UrQMD transport and the hybrid approach compared to the experimental data [1].

The first observable to look at is the charged particle multiplicity at midrapidity. In Fig. 1 the calculation of the centrality dependent multiplicity scaled by the number of participants (estimated in a Glauber approach) is shown. The hadronic transport approach UrQMD provides a reasonable description of the multiplicity. For central collisions the predictions published in [39] are right on top of the ALICE data while with decreasing centrality the number of charged particles is a little lower than in the data. This fair agreement with the data hints to the fact that the main particle production can be described by the initial binary nucleon-nucleon interactions treated by PYTHIA.

The hydrodynamic evolution with a hadron gas equation of state (Hybrid-HG) has only minor effects on the particle production. The multiplicities are very similar to the ones from the transport approach and the slightly higher yields can be understood from the entropy production when the system is forced to local equilibrium. Since ideal hydrodynamics implies an isentropic expansion this means that the charged particle multiplicity is mainly determined in the initial state and by the final resonance decays. For the hybrid calculation including deconfinement (Hybrid-DE) the yields of charged particles at midrapidity is roughly 20 % lower than in the hadronic case. This is due to the fact, that the pressure is higher in the early stages in the quark gluon plasma and therefore, the longitudinal expansion is more rapid than in the hadronic scenario. Therefore, employing the same freeze-out criterion for both calculations leads to lower particle yields at midrapidity in the hybrid calculation including a quark gluon plasma phase.

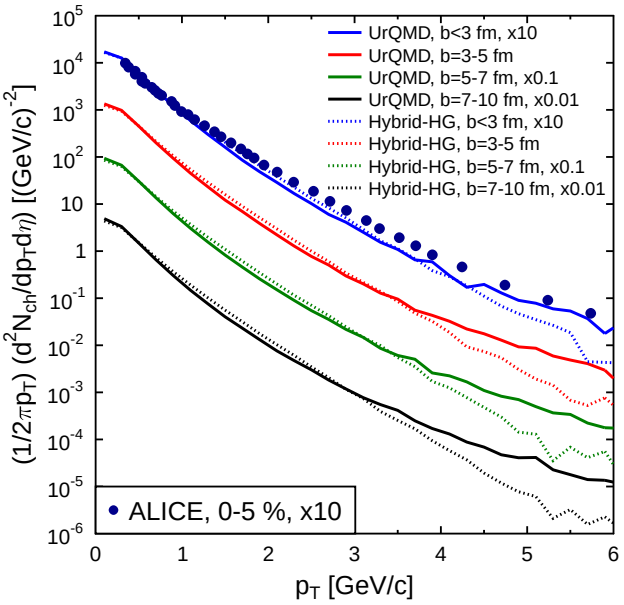

FIG. 2: (Color online) Transverse momentum spectra of charged particles for four different centralities calculated in the UrQMD transport and the hybrid approach compared to the available experimental data [2]. The lines are ordered according to decreasing centrality from top to bottom.

For the following calculations of spectra and collective flow four different centrality classes have been chosen that match the ones applied by the ALICE collaboration as they are listed in the following table:

Centrality class	Impact parameter range
0-5%	$b < 3$ fm
5-10%	$b = 3 - 5$ fm
10-20%	$b = 5 - 7$ fm
20-40%	$b = 7 - 10$ fm

The transverse momentum spectrum for charged particles in the mentioned centrality classes are compared to experimental data in the most central bin (see Fig. 2). The main difference between the hybrid and the transport calculation is in the slopes of the spectra. As expected the hydrodynamic evolution leads to a purely exponential p_T dependence which describes the data until $p_T < 3$ GeV very well. At higher transverse momenta the power law tail from hard processes becomes impor-

tant for a good agreement with the measured values. In the range from 4 to 6 GeV the non-equilibrium description exemplified by the UrQMD calculation provides a better description of the experimental data.

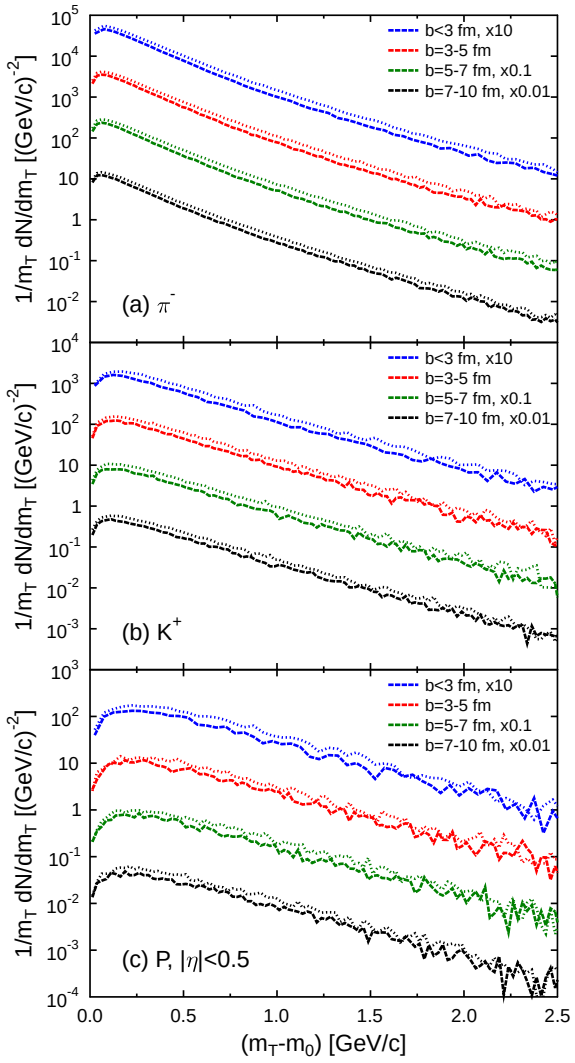

FIG. 3: (Color online) Transverse mass spectra of negative pions (a), positive kaons (b) and protons (c) for four different centralities calculated in the hybrid approach with two different equations of state where the dotted line represents the hadron gas (HG) and the dashed line the one with deconfined phase (DE). The lines are ordered according to decreasing centrality from top to bottom.

In Fig. 3 predictions for the transverse mass spectra at midrapidity of pions (a), kaons (b) and protons (c) are presented. The pion spectra are very similar to the charged particle spectra since they represent the major fraction of the newly produced particles in the collision. Kaons are strange mesons and protons are chosen because they have a higher mass and are baryonic degrees of freedom. The general features of the transverse mass spectra are similar to the ones observed at RHIC and imply a collective radial velocity that drives all the particle species. The two different equations of state lead to very similar results with the deconfinement transition having a little steeper slope due to the more rapid expansion due to the higher pressure in the quark gluon plasma phase. As it has been already shown in Fig. 1 the faster longitudinal expansion together with the same freeze-out transition criterion leads to lower particle yields at midrapidity in the hybrid calculation with deconfinement which is also visible in the transverse mass spectra.

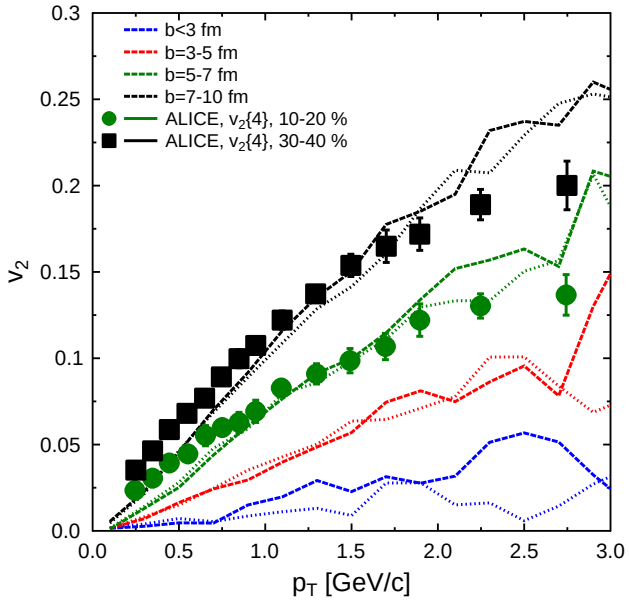

FIG. 4: (Color online) Elliptic flow of charged particles as a function of transverse momentum for four different centralities calculated in the hybrid approach with two different equations of state where the dotted line represents the hadron gas (HG) and the dashed line the one with deconfined phase (DE) compared to the experimental data[3]. The lines are ordered according to increasing centrality from top to bottom.

After proving a rather successful agreement with basic quantities like the multiplicity and transverse momentum spectrum the next step is to look at anisotropic flow observables. The elliptic flow has been calculated with respect to the reaction plane by averaging over all charged particles in all events to be compared to the ALICE measurement that relies on the four-particle cumulant method in two centrality bins. Fig. 4 shows a good agreement between the hybrid calculations and the data, especially between p_T=0.8-2.5 GeV. In the very low transverse momentum region the hybrid approach underpredicts the data which has been observed in other calculations as well [14]. At higher p_T again the influence of hard processes needs to be taken into account.

To quantify the shape of the initial conditions employed for the hydrodynamic calculation and its event-by-event fluctuations Fig. 5 shows the probability distribution of the coordinate space asymmetry characterized by

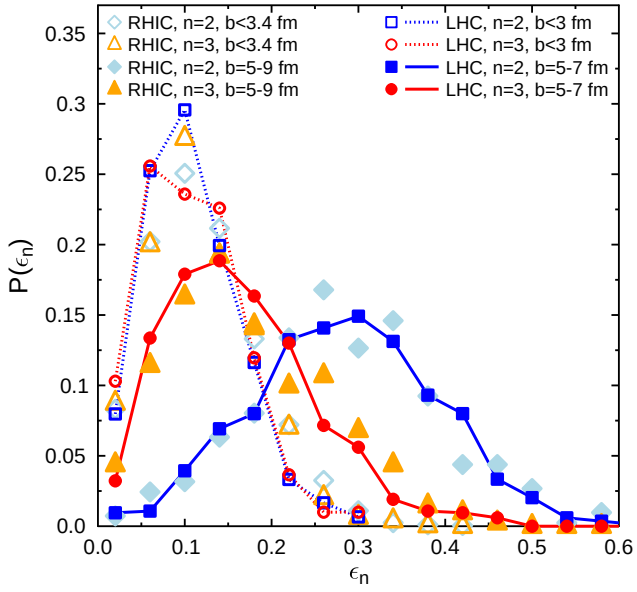

FIG. 5: (Color online) Probability distributions of the eccentricity coefficients (ϵ_2/ϵ_3) in the UrQMD initial state.The diamonds and triangles indicate the corresponding distributions for Au+Au collisions at RHIC at $\sqrt{s_{\rm NN}} = 200$ GeV.

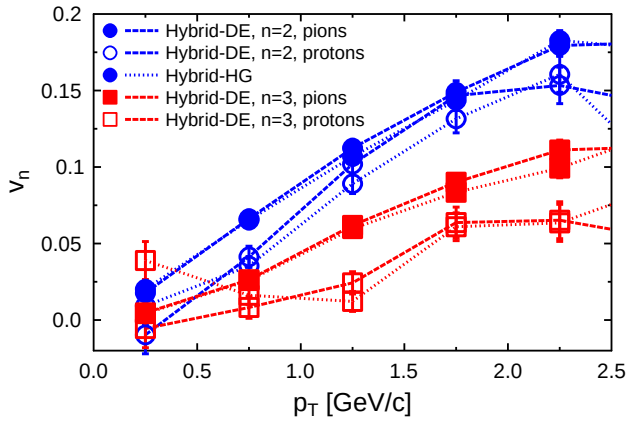

FIG. 6: (Color online) Triangular flow indicated by squares of pions (filled symbols) and protons (open symbols) as a function of transverse momentum compared to the corresponding elliptic flow result shown as circles calculated in the hybrid approach with two different equations of state (dashed and dotted line) for minimum bias Pb+Pb collisions at $\sqrt{s_{\rm NN}} = 2.76$ TeV.

the eccentricity and the triangularity as defined in [26]. The initial ϵ_n coefficients have been calculated in each event from the initially produced particles in UrQMD, before they are translated to the initial distributions for the hydrodynamics evolution. The normalized probability distribution is plotted for two different centrality bins.

For central collisions the mean value and the shape of the distributions are very similar for the participant eccentricity and the triangularity since both of them are mainly generated by fluctuations. For more peripheral collisions the eccentricity is influenced by a large geometry component due to the ellipsoidal shape of the initial state in the transverse plane. Therefore, the mean eccentricity is larger and the fluctuations increase leading to a wider distribution, whereas the triangularity stays smaller and the distribution has a smaller width.

Since the triangularity has been introduced because of its sensitivity to initial state fluctuations the higher multiplicity at LHC energies triggers the expectations that the fluctuations become smaller compared to RHIC energies. In Fig. 5 the triangles and diamonds depict the eccentricity and triangularity calculation from UrQMD initial conditions for Au+Au collisions at $E_{\rm cm} = 200A$ GeV. The ϵ_n distributions match almost exactly the ones at LHC energies for the two similar centrality classes. There are two possible explanations for this finding: Either this result indicates that the fluctuations in the energy deposition in the binary collisions is larger at LHC energies and compensates the smoothing from the higher number of particles or the eccentricity and triangularity are mainly sensitive to the geometry of the initial state that is given by the sampling of Woods-Saxon profiles for the nuclei which is very similar in Au+Au at RHIC and Pb+Pb at LHC.

To calculate the transverse momentum dependence of the anisotropic flow coefficients for identified particles (see Fig. 6) the event plane method including removal of auto-correlations and resolution correction has been applied as described in more detail in [26]. In this way, the predictions can be directly compared to a future experimental result for minimum bias Pb+Pb collisions at $E_{\rm cm} = 2.76A$ TeV. Both elliptic and triangular flow show the expected mass splitting between pions and protons. Furthermore, the elliptic flow has roughly double the value of the triangular flow result as it has previously been calculated for RHIC energies. The anisotropic flow coefficients are not very sensitive to the choice of the equation of state which points to the fact that the interplay of freeze-out transition and flow development due to pressure gradients results in very similar values independent of the existence of a quark gluon plasma phase.

Finally in Fig. 7 predictions for the transverse momentum dependence of triangular flow for charged particles in the four different centrality classes are made. There is a weak centrality dependence, but overall the different curves from the hybrid calculation look very similar qualitatively. Since the calculation with the deconfinement phase transition leads to very similar results, only the hadron gas result is shown in this figure to reduce the number of lines displayed. To investigate the effect of a finite viscosity during the expansion the calculation is compared to the pure UrQMD result. Within the very viscous hadronic transport approach the pressure gradi-

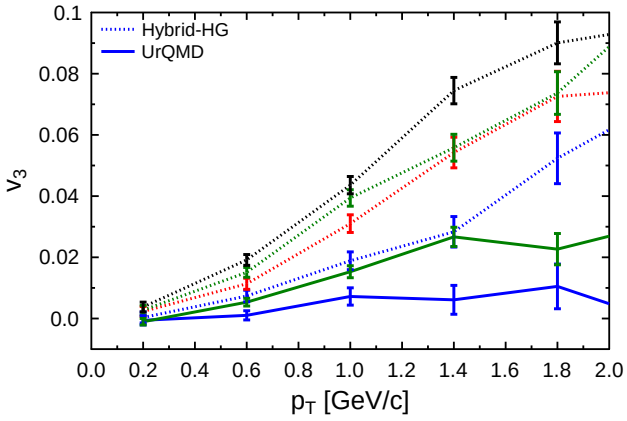

FIG. 7: (Color online) Triangular flow of charged particles as a function of transverse momentum calculated in the hybrid approach for four different centrality classes of Pb+Pb collisions at $\sqrt{s_{\rm NN}} = 2.76$ TeV compared in two centrality bins to the corresponding results of the UrQMD transport approach where the lower full line indicates central collisions and the upper full line represents mid-central collisions. The dotted lines are ordered according to increasing centrality from top to bottom.

ents are too small to transfer the initial coordinate space asymmetry to a final state momentum space asymmetry. For impact parameters up to $b = 5$ fm the result is consistent with zero and even for very peripheral event the result is negligible especially in the low transverse momentum region where most of the particles are. This leads to the conclusion that a finite triangular flow measurement is a strong indication for almost ideal hydrodynamic behavior during the hot and dense evolution of the heavy ion reaction.

To summarize we have presented a comparison of bulk observables measured in Pb+Pb collisions at $E_{\rm cm} = 2.76A$ TeV to a state-of-the-art event-by-event hybrid description. Employing the same parameters as have been used for Au+Au collisions at RHIC a reasonably good agreement for the multiplicity, transverse momentum spectra and elliptic flow is achieved. One can conclude that the basic assumptions about the major ingredients that are needed to describe the dynamic evolution of heavy ion reactions do not have to be revised at LHC energies.

With a non-equilibrium initial state, an ideal hydrodynamic evolution and a hadronic afterburner predictions for identified particle transverse mass spectra and elliptic as well as triangular flow are made. The initial state fluctuations quantified by the probability distribution of the initial eccentricity and triangularity are very similar at LHC and RHIC energies within the UrQMD approach. A large viscosity during the evolution results in almost negligible higher harmonic coefficients, so the triangular flow measurement at LHC will provide a robust confirmation of the almost ideal hydrodynamic expansion.

Acknowledgements

We are grateful to the Open Science Grid for the computing resources. The author thanks Dirk Rischke for providing the 1 fluid hydrodynamics code. H.P. acknowledges support by the Feodor Lynen program of the Alexander von Humboldt Foundation. This work was supported in part by U.S. department of Energy grant DE-FG02-05ER41367. H.P. thanks Jan Steinheimer for help with the extension of the equation of state, Guangyou Qin for providing the Glauber calculation of the numebr of particpants and Steffen A. Bass and Berndt Müller for fruitful discussions.

[1] K. Aamodt *et al.* [ALICE Collaboration], Phys. Rev. Lett. **106**, 032301 (2011).
[2] K. Aamodt *et al.* [ALICE Collaboration], Phys. Lett. B **696**, 30 (2011).
[3] K. Aamodt *et al.* [The ALICE Collaboration], arXiv:1011.3914 [nucl-ex].
[4] K. Aamodt *et al.* [The ALICE Collaboration], Phys. Rev. Lett. **105**, 252301 (2010).
[5] N. Armesto *et al.*, J. Phys. G **35**, 054001 (2008).
[6] M. Luzum, Phys. Rev. C **83**, 044911 (2011).
[7] H. Niemi, G. S. Denicol, P. Huovinen, E. Molnar and D. H. Rischke, arXiv:1101.2442 [nucl-th].
[8] H. Song, S. A. Bass and U. W. Heinz, arXiv:1103.2380 [nucl-th].
[9] R. A. Lacey, A. Taranenko, N. N. Ajitanand and J. M. Alexander, Phys. Rev. C **83**, 031901 (2011).
[10] S. A. Bass and A. Dumitru, Phys. Rev. C **61**, 064909 (2000).
[11] D. Teaney, J. Lauret and E. V. Shuryak, arXiv:nucl-th/0110037.
[12] T. Hirano, U. W. Heinz, D. Kharzeev, R. Lacey and Y. Nara, Phys. Lett. B **636**, 299 (2006).
[13] C. Nonaka and S. A. Bass, Phys. Rev. C **75**, 014902 (2007).
[14] T. Hirano, P. Huovinen and Y. Nara, arXiv:1012.3955 [nucl-th].
[15] B. Schenke, S. Jeon and C. Gale, arXiv:1102.0575 [hep-ph].
[16] R. Andrade, F. Grassi, Y. Hama, T. Kodama and O. . J. Socolowski, Phys. Rev. Lett. **97**, 202302 (2006).
[17] B. M. Tavares, H. J. Drescher and T. Kodama, Braz. J. Phys. **37**, 41 (2007).
[18] H. Petersen, J. Steinheimer, G. Burau, M. Bleicher and H. Stocker, Phys. Rev. C **78**, 044901 (2008).
[19] H. Holopainen, H. Niemi and K. J. Eskola, Phys. Rev. C **83**, 034901 (2011).
[20] K. Werner, I. Karpenko, T. Pierog, M. Bleicher and K. Mikhailov, Phys. Rev. C **82**, 044904 (2010).
[21] B. Schenke, S. Jeon and C. Gale, Phys. Rev. Lett. **106**, 042301 (2011).

[22] Z. Qiu, U. W. Heinz, [arXiv:1104.0650 [nucl-th]].
[23] T. Renk, H. Holopainen, R. Paatelainen and K. J. Eskola, arXiv:1103.5308 [hep-ph].
[24] H. Holopainen, S. Rasanen and K. J. Eskola, arXiv:1104.5371 [hep-ph].
[25] H. Petersen, T. Renk and S. A. Bass, Phys. Rev. C **83**, 014916 (2011).
[26] H. Petersen, G. Y. Qin, S. A. Bass and B. Muller, Phys. Rev. C **82**, 041901 (2010).
[27] H. Petersen, C. Coleman-Smith, S. A. Bass and R. Wolpert, J. Phys. G **38**, 045102 (2011).
[28] S. A. Bass *et al.*, Prog. Part. Nucl. Phys. **41**, 255 (1998).
[29] M. Bleicher *et al.*, J. Phys. G **25**, 1859 (1999).
[30] H. Petersen, M. Bleicher, S. A. Bass and H. Stocker, arXiv:0805.0567 [hep-ph].
[31] B. Nilsson-Almqvist and E. Stenlund, Comput. Phys. Commun. **43**, 387 (1987).
[32] T. Sjostrand, Comput. Phys. Commun. **82**, 74 (1994).
[33] D. H. Rischke, S. Bernard and J. A. Maruhn, Nucl. Phys. A **595**, 346 (1995).
[34] D. H. Rischke, Y. Pursun and J. A. Maruhn, Nucl. Phys. A **595**, 383 (1995) [Erratum-ibid. A **596**, 717 (1996)].
[35] J. Steinheimer, V. Dexheimer, H. Petersen, M. Bleicher, S. Schramm and H. Stoecker, Phys. Rev. C **81**, 044913 (2010).
[36] J. Steinheimer, S. Schramm, H. Stocker, J. Phys. G **G38**, 035001 (2011).
[37] Y. Aoki, G. Endrodi, Z. Fodor, S. D. Katz, K. K. Szabo, Nature **443**, 675-678 (2006).
[38] H. Petersen, J. Steinheimer, M. Bleicher and H. Stocker, J. Phys. G **36**, 055104 (2009).
[39] M. Mitrovski, T. Schuster, G. Graf, H. Petersen and M. Bleicher, Phys. Rev. C **79**, 044901 (2009).